Progress In Electromagnetics Research M, Vol. 91, 155–164, 2020

2D-FDTD Method to Estimate the Complex Permittivity of a Multilayer Dielectric Materials at Ku-Band Frequencies

Lahcen Ait Benali[1, *], Jaouad Terhzaz[2], Abdelwahed Tribak[1], and Angel Mediavilla[3]

Abstract—In this paper, a new measurement method is proposed to estimate the complex permittivity for each layer in a multi-layer dielectric material using a Ku-band rectangular waveguide WR62. The S_{ij}-parameters at the reference planes in the rectangular waveguide loaded by a multi-layer material sample are measured as a function of frequency using the E8634A Network Analyzer. Also, by applying the two-dimensional finite difference in time domain (2D-FDTD), the expressions for these parameters as a function of complex permittivity of each layer are calculated. The Nelder-Mead algorithm is then used to estimate the complex permittivity of each layer by matching the measured and calculated S_{ij}-parameters. This method has been validated by estimating, at the Ku-band, the complex permittivity of each layer of three bi-layer and one tri-layer dielectric materials. A comparison of estimated values of the complex permittivity obtained from multi-layer measurements and mono-layer measurements is presented.

1. INTRODUCTION

Application of multi-layer dielectric materials in microwave integrated circuits, monolithic microwave integrated circuits, and communication industries requires the exact knowledge of the complex permittivity of each layer of multi-layer materials [1, 2]. By choosing the electromagnetic properties and appropriate thickness for each layer, it is possible to synthesize multi-layer dielectric materials with new electromagnetic properties otherwise not found in a single mono-layer dielectric material [3]. Waveguides techniques are widely used to determine the complex permittivity of multilayer dielectric material over Ku-band frequencies [3, 4]. The characterization technique is chosen according to the frequency band used and the physical properties of the material to be characterized. Several techniques have been developed and used to determine the complex permittivity of single-layer dielectric materials. Free space methods, cavity resonator techniques, and transmission line or waveguide techniques [4, 5] are among these techniques. Each technique has its distinct advantages and drawbacks. For measurements of complex permittivity of material over a wideband of frequencies, transmission line or waveguide techniques are widely used [3, 6], these methods are more accurate than free space technique but are less accurate than the resonant cavity technique. In a waveguide measurement method, the S_{ij}-parameters of sample holder loaded with a mono-layer material sample is measured by a network analyzer and calculated as a function of complex permittivity of the material by using a simple waveguide modal expansion method. To determine the complex permittivity of the sample of mono-layer material, the inverse procedure is used which matches the calculated and measured values of the S_{ij}-parameters of the sample holder [7, 8]. A sample holder loaded with a sample of monolayer or bi-layer material is preferred so that the modal analysis is sufficient and accurate in order to determine the S_{ij}-parameters of the sample holder [9–11]. However, when the sample holder is loaded with a multi-layer material, the complete modal analysis to accurately determine the complex permittivity of each layer of the

Received 1 February 2020, Accepted 9 April 2020, Scheduled 20 April 2020
* Corresponding author: Lahcen Ait Benali (aitbenalilahcen@hotmail.fr).
[1] INPT, Rabat, Morocco. [2] CRMEF, Casablanca, Morocco. [3] DICOM, University of Cantabria, Santander, Spain.

multi-layer material is very complicated. The problem of electromagnetic wave propagation inside waveguide which is loaded with a multilayer dielectric material has been the subject of many research works in recent years [8, 10]. Several methods have been used to solve electromagnetic structures in the frequency domain such as Finite Element Method (FEM), Mode Matching Technique (MMT) [10], and the Finite-Difference Time Domain method (FDTD) [11]. The FDTD method has the advantage over other numerical methods in that it does not use empirical approximations.

In this work, the 2D FDTD method combined with Nelder-Mead algorithm is proposed to determine the complex permittivity of each layer for a multi-layer material using a Ku-band rectangular waveguide. The S_{ij}-parameters at the reference planes in the rectangular waveguide WR62 loaded by a multi-layer material sample are measured as a function of frequency using the E8634A Network Analyzer. The 2D FDTD method is used to analyze the discontinuities created by a multi-layer material placed in rectangular waveguide sample in order to determine the expressions of the S_{ij}-parameters as a function of complex permittivity of each layer for a multi-layer material. The Nelder-Mead algorithm is then used to estimate the complex permittivity of each layer by matching the measured and calculated S_{ij}-parameters of the rectangular waveguide sample holder. This method has been validated by estimating, at the Ku-band, the complex permittivity of each layer of bi-layer and tri-layer dielectric materials. Also, the results of determining the complex permittivities of each layer obtained from single-layer measurements are compared with those obtained from multi-layer measurements.

2. THEORY

2.1. Direct Problem

This section presents the calculation of the S_{ij}-parameters of a rectangular waveguide loaded with a multi-layer dielectric material as shown in Fig. 1.

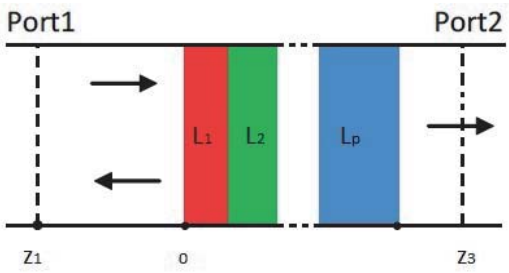

Figure 1. Rectangular waveguide loaded with a Multi-layer dielectric material.

The multi-layer dielectric material consists of p layers, where the first layer has complex permittivity ε_{r1} and is located between transverse planes $z = 0$ and $z = L_1$. The second layer has complex permittivity ε_{r2} and is located between transverse planes $z = L_1$ and $z = L_1 + L_2$, and the third layer has complex permittivity ε_{r3} and is located between $z = L_1 + L_2$ and $z = L_1 + L_2 + L_3$, etc.

It is assumed that the waveguide is excited by a dominant TE_{10} mode. The electric field inside rectangular waveguide is obtained using 2D-FDTD method. The 2D-FDTD formulation is based on the direct discretization of Maxwell's equations given by:

$$\frac{\partial \vec{H}}{\partial t} = -\frac{1}{\mu}\vec{\nabla} \times \vec{E} \tag{1}$$

$$\frac{\partial \vec{E}}{\partial t} = \frac{1}{\varepsilon}\vec{\nabla} \times \vec{H} \tag{2}$$

where ε and μ represent the complex permittivity and complex permeability, respectively. In Cartesian coordinates and following Yee's notation [8], we obtain the two-dimensional FDTD formulation, for the components E_y, H_x, and H_z of Equations (4) and (5):

$$E_y^{n+1}(i,k) = E_y^n(i,k) + \frac{\Delta t}{\varepsilon_0 \varepsilon_r \Delta z}\left[H_x^{n+\frac{1}{2}}(i,k) - H_x^{n+\frac{1}{2}}(i,k-1)\right]$$

$$-\frac{\Delta t}{\varepsilon_0\varepsilon_r\Delta x}\left[H_z^{n+\frac{1}{2}}(i,k)-H_z^{n+\frac{1}{2}}(i-1,k)\right] \tag{3}$$

$$H_x^{n+\frac{1}{2}}(i,k) = H_x^{n-\frac{1}{2}}(i,k)+\frac{\Delta t}{\mu_0\mu_r\Delta z}\left[E_y^n(i,k+1)-E_y^n(i,k)\right] \tag{4}$$

$$H_z^{n+\frac{1}{2}}(i,k) = H_z^{n-\frac{1}{2}}(i,k)-\frac{\Delta t}{\mu_0\mu_r\Delta z}\left[E_y^n(i+1,k)-E_y^n(i,k)\right] \tag{5}$$

where ε_r is the relative complex permittivity, and μ_r is the relative complex permeability. Δx and Δz are the space steps following two directions x and z, and Δt is the temporal step. In order to ensure the precision of the derivative space implied in the calculation of the electrical field components, it is necessary that the mesh sizes of network FDTD are selected so as to be sufficiently small compared to the wavelength in waveguide [7, 8].

$$\mathrm{Max}(\Delta x,\Delta z)<\frac{\lambda_{g\min}}{m_0} \tag{6}$$

where $10<m_0<100$, and $\lambda_{g\min}$ is the lowest wavelength in the rectangular waveguide.

To ensure the numerical stability of algorithm 2D FDTD, it is necessary that the increments Δt, Δx, and Δz satisfy a stability condition [7, 8]:

$$\Delta t\le\frac{1}{c}\left(\frac{1}{\Delta x^2}+\frac{1}{\Delta z^2}\right)^{-\frac{1}{2}} \tag{7}$$

where c is the velocity of light in the vacuum.

Two absorbing planes are required in the waveguide region, behind the waveguide input plane and after the output plane. We have to set an absorbing boundary condition to the mesh to be truncated by means of an artificial boundary which simulates the unbounded surroundings. The absorbing boundary in the z direction is given by equations:

$$E_y^{n+1}(i,0) = E_y^n(i,1)+\frac{c\Delta t-\Delta z}{c\Delta t+\Delta z}\left[E_y^{n+1}(i,1)-E_y^n(i,0)\right] \tag{8}$$

$$E_y^{n+1}(i,k_{\max}) = E_y^n(i,k_{\max}-1)+\frac{c\Delta t-\Delta z}{c\Delta t+\Delta z}\left[E_y^{n+1}(i,k_{\max})-E_y^n(i,k_{\max}-1)\right] \tag{9}$$

If the position of the absorbing boundary and input waveguide are chosen so that merely the fundamental mode could propagate there, the influence of the higher order modes in the input waveguide can be neglected. The selected input port is then excited by its modal (in our case, fundamental mode TE_{10}) field distribution. To calculate the reflection coefficient at the reference plane of the rectangular waveguide on the Ku-band frequencies, an excitation with a sinusoidally modulated Gaussian pulse is utilized:

$$E_y\left(i,k_{source}\right)=e^{-\frac{(t-t_0)^2}{\tau^2}}\sin(\omega_0 t)\sin\left(\frac{\pi i\Delta x}{a}\right) \tag{10}$$

After an appropriate number of time iterations n_t, a stable distribution is obtained, and the DFT algorithm can be applied in order to yield the desired complex field amplitude coefficients at the corresponding frequency.

We obtain the S_{ij} parameters for the TE_{10} mode by following the method described in [10]. The magnitude and phase of the mode amplitudes A and B are determined by applying the relation:

$$\int_0^a E_y(x,z_1)\cdot H_x(TE_{10})dx = w_1 = A(z_1)+B(z_1) \tag{11}$$

$$\int_0^a E_y(x,z_2=z_1+\Delta z)\cdot H_x(TE_{10})dx = w_2 = A(z_1)e^{-j\gamma\Delta z}+B(z_1)e^{j\gamma\Delta z} \tag{12}$$

$$\int_0^a E_y(x,z_3)\cdot H_x(TE_{10})dx = w_3 = A(z_3) \tag{13}$$

where $H_x(TE_{10}) = \sin(\pi \cdot x/a)$ is the normalized modal magnetic field, and $\gamma = \sqrt{(\frac{\omega}{c})^2 - (\frac{\pi}{a})^2}$ is the modal propagation constant. Using Equations (11), (12), and (13) yields:

$$S_{11} = \frac{B(z_1)}{A(z_1)} = \frac{w_2 - w_1 e^{-j\gamma\Delta z}}{w_1 e^{j\gamma\Delta z} - w_2} \tag{14}$$

$$S_{21} = \frac{A(z_3)}{A(z_1)} = w_3 \frac{e^{j\gamma\Delta z} - e^{-j\gamma\Delta z}}{w_1 e^{j\gamma\Delta z} - w_2} \tag{15}$$

To calculate S_{22} and S_{12}, we follow the same procedure by inverting the excitation plane in the waveguide.

2.2. Inverse Problem

This section presents the calculation of the complex permittivity for each layer in a multi-layer dielectric material given with specific prior knowledge of the thickness of each layer. For this reason, we use the Fminsearch function implemented in MATLAB [12] which is based on the Nelder-Mead sequential simplex algorithm [13]. This function solves nonlinear unconstrained multi-variable optimization problems, which finds the minimum of a scalar function of several variables from an initial guess of the complex relative permittivity such as $\varepsilon'_r = 1.5$, $\varepsilon''_r = 0.005\varepsilon'_r$. The error function that we want to minimize with Fminsearch function is the square sums of errors between the measured and calculated S_{ij}-parameters written as follows:

$$f(\varepsilon_{r1}, \varepsilon_{r2}, \ldots, \varepsilon_{rp}) = \sum_{ij} |S_{ijc} - S_{ijm}|^2 \tag{16}$$

3. NUMERICAL RESULTS

3.1. Direct Problem

To validate the direct problem, the S_{ij}-parameters at the reference planes of the rectangular waveguide in Ku-band loaded by a mono-layer dielectric material Teflon ($\varepsilon'_r = 2.08$, $\varepsilon''_r = 0.002$) with thickness $L = 2\,\text{mm}$ are calculated using the procedure described in 2.1 where $\Delta x = 0.7524\,\text{mm}$, $\Delta z = 0.4\,\text{mm}$, $\Delta t = 1.1663\ 10^{-12}\,\text{s}$, and $n_t = 1500$ are also simulated with HFSS (High Frequency Structure Simulator) software as shown in Fig. 2. It is seen, from these results, that there is an excellent agreement between calculated and simulated S_{ij}-parameters.

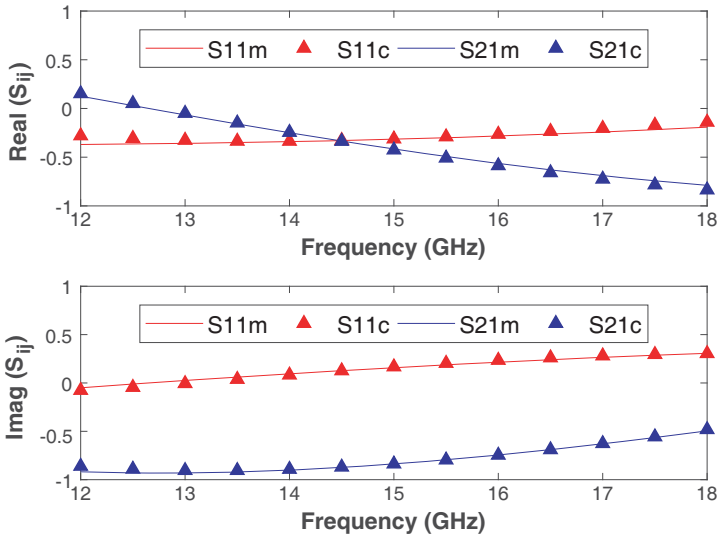

Figure 2. Simulated and calculated S_{ij}-parameters in a rectangular waveguide WR62 ($2L_0 + L = 6.8\,\text{mm}$) loaded by Teflon with thickness $L = 2\,\text{mm}$.

To validate the direct problem of bi-layer dielectric material, the S_{ij}-parameters of a rectangular waveguide in Ku-band loaded by a bi-layer dielectric material formed by FR4 Epoxy ($\varepsilon_{r2} = 4.5 - j0.090$) with thickness $L_2 = 1.6\,\text{mm}$ and Teflon ($\varepsilon_{r1} = 2.08 - j0.002$) with thickness $L_1 = 2\,\text{mm}$ are calculated using the procedure described in Section 2.1 and simulated by the use of HFSS software. As can be seen from the results shown in Fig. 3, there is a good agreement between calculated and simulated S_{ij}-parameters.

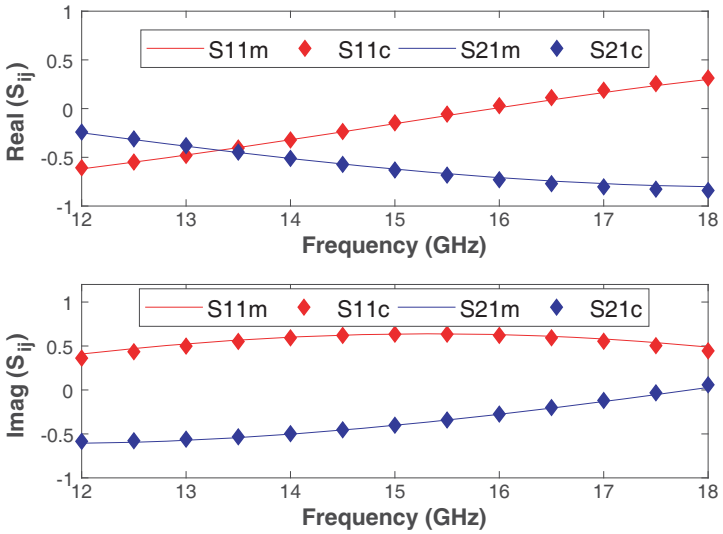

Figure 3. Simulated and calculated S_{ij}-parameters in a rectangular waveguide ($2L_0+L_1+L_2 = 6.8\,\text{mm}$) loaded by a bi-layer FR4 (1.6 mm) and Teflon (2 mm).

Then the direct problem of tri-layer dielectric material is validated, and the S_{ij}-parameters of a rectangular waveguide in Ku-band loaded by a tri-layer dielectric material formed by Teflon ($\varepsilon_{r1} = 2.08 - j0.002$) with thickness $L_1 = 2\,\text{mm}$ and FR4 Epoxy ($\varepsilon_{r2} = 4.5 - j0.090$) with thickness $L_2 = 1.6\,\text{mm}$ and Delrin ($\varepsilon_{r1} = 2.9 - j0.044$) with thickness $L_3 = 2.4\,\text{mm}$ are calculated using the procedure described in Section 2.1 and simulated by the use of HFSS software. As can be seen from the results shown in Fig. 4, there is a good agreement between calculated and simulated S_{ij}-parameters.

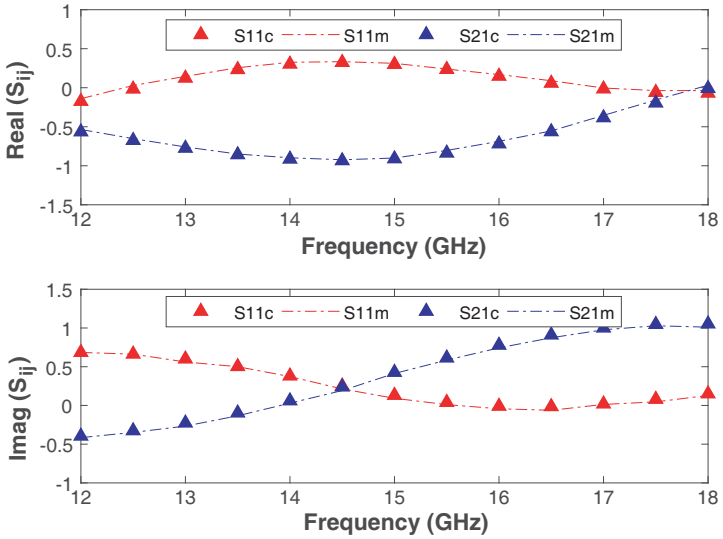

Figure 4. Simulated and calculated S_{ij}-parameters in a rectangular waveguide ($2L_0 + L_1 + L_2 + L_3 = 6.8\,\text{mm}$) loaded by a Tri-layer Teflon (2 mm), FR4 (1.6 mm) and Delrin (2.4 mm).

3.2. Inverse Problem

For the inverse problem, using the procedure described in Sections 2.1 and 2.2, the complex permittivity of mono-layer dielectric material and of each layer in a bi-layer dielectric material was determined in the Ku-band frequencies.

We consider the measurement system shown in Fig. 5. The S_{ij}-parameters at the references plane of a Ku-band rectangular waveguide WR62 loaded by a mono or a bi-layer dielectric material were measured using the E8634A Network Analyzer.

Figure 5. The measurement system.

First of all, we applied this method to estimate the complex permittivity of mono-layer dielectric material which was determined in the Ku-band frequencies. The initial guess of the complex permittivity was $\varepsilon_r = 1.5(1 - j0.005)$. The values of complex permittivity of Teflon, FR4 epoxy, and Delrin, with thicknesses of 2 mm, 1.6 mm, and 2 mm, respectively, were determined. For all cases, the obtained results are plotted in Fig. 6.

The results obtained for the complex permittivity of mono-layers by using the procedure described

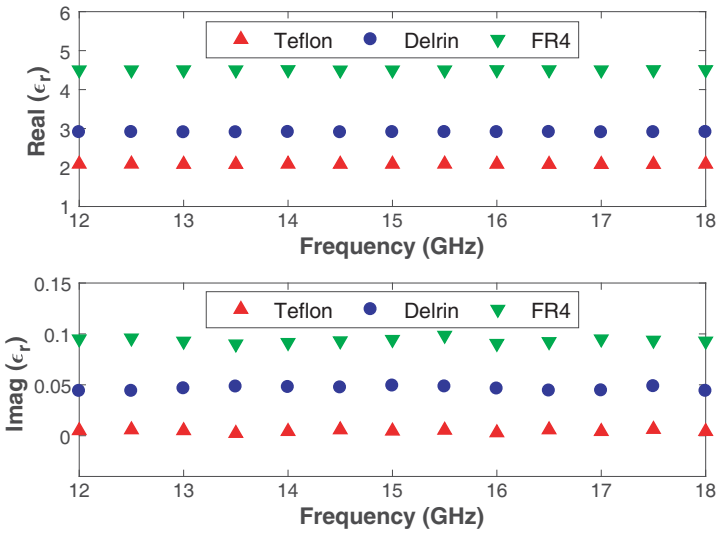

Figure 6. Complex permittivity of the mono-layers Teflon (2 mm), Delrin (2 mm) and FR4 (1.6 mm) obtained from the S_{ij} measured using the inverse procedure with Nelder-Mead algorithm.

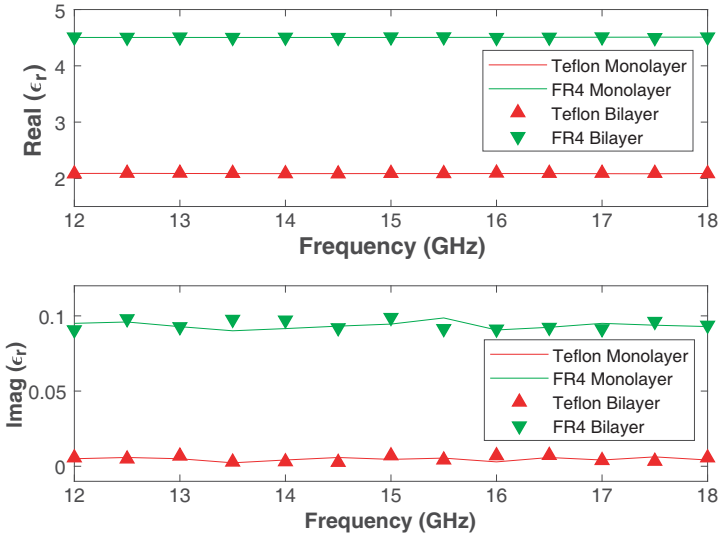

Figure 7. Complex permittivity for each layer in the bi-layer FR4 epoxy (1.6 mm)-Teflon (2 mm) obtained from the S_{ij} measured using the inverse procedure with Nelder-Mead algorithm.

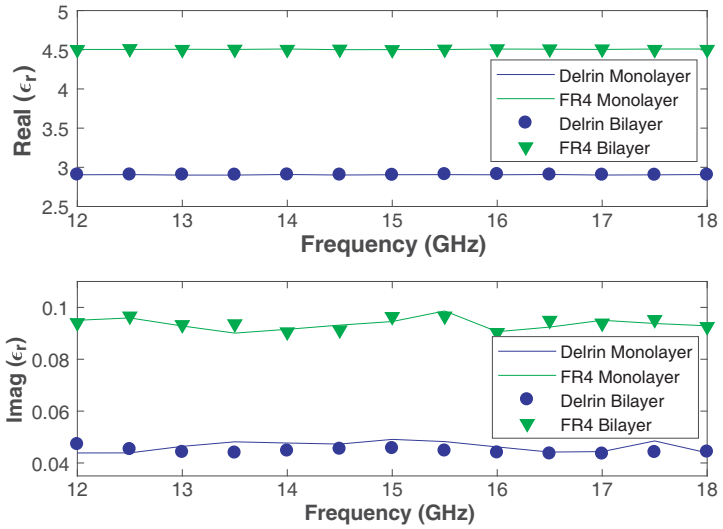

Figure 8. Complex permittivity for each layer in the bi-layer FR4 epoxy (1.6 mm)-Delrin (2 mm) obtained from the S_{ij} measured using the inverse procedure with Nelder-Mead algorithm.

in this work are in good agreement with [14]. We can see that FR4 is a dielectric material with loss tangent about 0.02. However, the Teflon dielectric has a small loss tangent which is around 0.001. For the inverse problem, using the procedure described in Sections 2.1 and 2.2, the complex permittivity for each layer in the bi-layer dielectric material was determined in the Ku-band frequencies. The initial guess of the complex permittivity was $\varepsilon'_{r1} = \varepsilon'_{r2} = 1.5$, $\varepsilon''_{r1} = 0.005\varepsilon'_{r1}$, and $\varepsilon''_{r2} = 0.01\varepsilon'_{r2}$. The values of dielectric permittivity for each layer in the bi-layer FR4 epoxy-Teflon are determined and plotted in Fig. 7. Those of FR4 epoxy-Delrin are in Fig. 8, and those of Teflon-Delrin are in Fig. 9.

From the results depicted in Figs. 7–9, we can conclude that there is a good agreement between the values of the complex permittivities of the mono-layers materials and those of each layer of the bi-layer materials made up from these mono-layers materials.

Table 1 presents the average values and average relative errors of the complex permittivities of each layer of material samples in the Ku-band calculated from monolayer and bi-layer measurements.

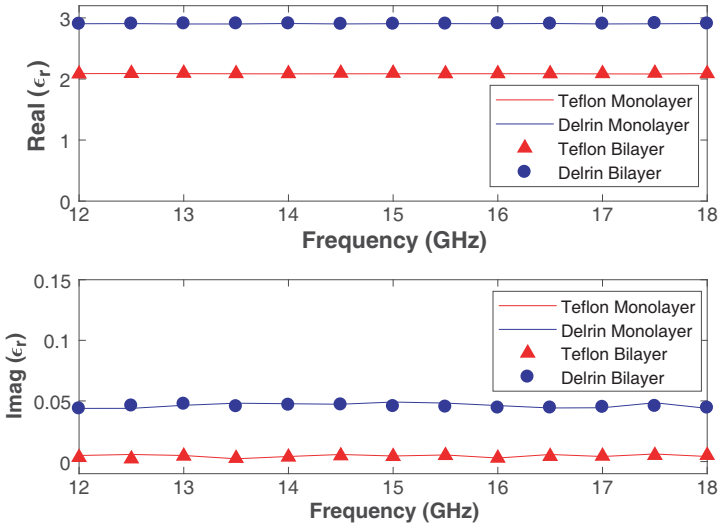

Figure 9. Complex permittivity for each layer in the bi-layer Teflon (2 mm)-Delrin (2 mm) obtained from the S_{ij} measured using the inverse procedure with Nelder-Mead algorithm.

Table 1. Average complex permittivity and average relative error percentage on the real and imaginary parts of the complex permittivity at Ku-band obtained for a Bilayer dielectric material.

Materials		Measurement		% Error	
Bilayer	Monolayer	Monolayer	Bilayer	ε_r'	ε_r''
FR4-Teflon	FR4	$4.5058 - j0.0936$	$4.5081 - j0.0941$	$< 1\%$	$< 4.5\%$
	Teflon	$2.0851 - j0.0047$	$2.0880 - j0.0049$		
FR4-Delrin	FR4	$4.5058 - j0.0936$	$4.5021 - j0.0938$		
	Delrin	$2.9047 - j0.0463$	$2.9066 - j0.0447$		
Teflon-Delrin	Delrin	$2.9047 - j0.0463$	$2.9078 - j0.0455$		
	Teflon	$2.0851 - j0.0047$	$2.0895 - j0.0045$		

The results presented in Table 1 show a good agreement between the average values of the complex permittivities of each layer obtained from the monolayer measurements and those obtained from the bilayer measurements with a small average relative error at the real part of the complex permittivity (lower than 1%), and this error can be explained by the presence of air gaps between the individual layers in the bi-layer materials. Because of the low losses of the materials studied, this error can be scarcely higher at the imaginary part ($\leq 4.5\%$).

To examine the stability of the method, we present, in Table 2, the average values and average relative errors of the complex permittivities of each layer of material samples in the Ku-band calculated from a bi-layer measurements with $\pm 10\%$ relative error in thicknesses.

It is seen in Table 2 that the relative error in the real part of the complex permittivity is small ($\leq 5\%$), but in the imaginary part it can reach 8.6% for the Teflon with low loss.

At the end, in Fig. 10 we plot the results obtained for the complex permittivity for each layer in the tri-layer Teflon (2 mm)-FR4 (1.6 mm)-Delrin (2.4 mm) from the measured S_{ij}-parameters. The results presented in Table 3 show a good agreement between the average values of the complex permittivities of each layer obtained from the monolayer measurements and those obtained from the tri-layer measurements with a small average relative error at the real part of the complex permittivity (lower than 2%), and this error can be explained by the presence of air gaps between the individual layers in the tri-layer materials. Because of the low losses of the materials studied, this error can be scarcely higher at the imaginary part ($\leq 8.5\%$).

Table 2. Average values and average relative errors of the complex permittivities of each layer of material samples in the Ku-band calculated from a bi-layer measurements with ±10% relative error in thicknesses.

Material		Measurement	% Error	
Bilayer	Monolayer	ε_r	ε_r'	ε_r''
FR4 (1.6 mm)-Teflon (2.0 mm)	FR4	$4.5081 - j0.0941$	–	–
	Teflon	$2.0880 - j0.0049$	–	–
FR4 (1.8 mm)-Teflon (1.8 mm)	FR4	$4.2827 - j0.0913$	-5%	-3%
	Teflon	$2.1214 - j0.0053$	1.6%	8.6%
FR4 (1.4 mm)-Teflon (2.2 mm)	FR4	$4.6433 - j0.0958$	3%	1.8%
	Teflon	$2.1214 - j0.0050$	1.6%	1.6%

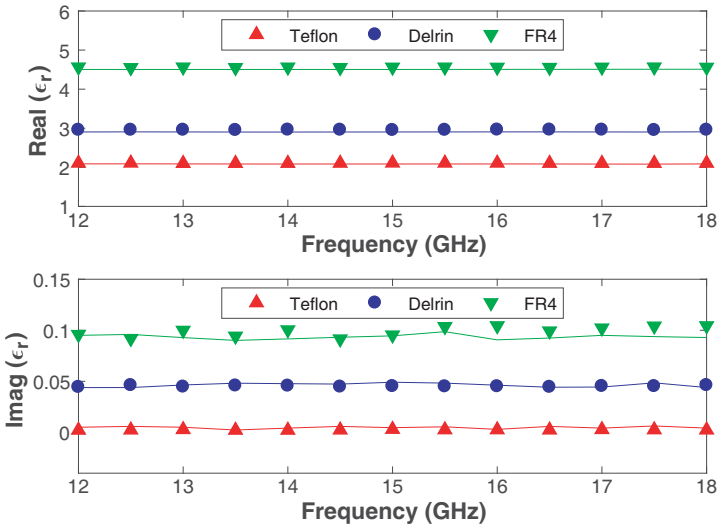

Figure 10. Complex permittivity for each layer in the tri-layer Teflon (2 mm)-FR4 (1.6 mm)-Delrin (2.4 mm) obtained from the S_{ij} measured using the inverse procedure with Nelder-Mead algorithm compared with the monolayer measurements results.

Table 3. Average complex permittivity and average relative error percentage on the real and imaginary parts of the complex permittivity at Ku-band obtained for a Trilayer dielectric material.

Materials		Measurement		% Error	
Trilayer	Monolayer	Monolayer	Trilayer	ε_r'	ε_r''
Teflon-FR4-Delrin	Teflon	$2.0851 - j0.0047$	$2.1046 - j0.0043$	1.0	8.5
	FR4	$4.5058 - j0.0936$	$4.5606 - j0.0990$	1.2	6
	Delrin	$2.9047 - j0.0463$	$2.9568 - j0.0452$	1.8	2.4

4. CONCLUSION

In this work, a new measurement method has been presented to estimate the complex permittivity of each layer in a multi-layer dielectric material with a specific prior knowledge of the thickness using a Ku-band rectangular waveguide WR62. The S_{ij}-parameters are measured by Vector Network Analyzer and calculated as a function of complex permittivity of each layer using 2D-FDTD method. The Nelder-Mead Algorithm has been used to estimate the complex relative permittivity of each layer in a

multi-layer dielectric material by matching the calculated value with measured value of S_{ij}-parameters of a Ku-band rectangular waveguide, loaded by a tri-layer (or a bi-layer) dielectric material. The results obtained from tri-layer measurement are in good agreement with those obtained from bi-layer and mono-layer measurement. This method has been validated using a tri-layer dielectric material such as FR4-Teflon-Delrin and bi-layer dielectric materials such as FR4-Teflon, FR4-Delrin, and Delrin-Teflon. The future work is to adapt this technique to estimate the complex permittivity of lossy materials and to estimate simultaneously the dielectric and the magnetic properties of magnetic materials.

REFERENCES

1. Gupta, K. and P. S. Hall, *Analysis and Design of Integrated Circuit-Antenna Modules*, 241–248, Wiley, 1999.
2. Chakravarty, S. and R. Mittra, "Application of the micro-genetic algorithm to the design of spatial filters with frequency-selective surfaces embedded in dielectric media," *IEEE Trans. Electromagn. Compat.*, Vol. 44, No. 2, 338–346, 2002.
3. Deshpande, M. D. and K. Dudley, *Estimation of Complex Permittivity of Composite Multilayer Material at Microwave Frequency Using Waveguide Measurements*, 212–398, NASA Langley Res, 2003.
4. Ghodgaonkar, D. K., V. V. Varadan, and V. K. Varadan, "A freespace method for measurement of dielectric constants and loss tangents at microwave frequencies," *IEEE Trans. Instrum. Meas.*, Vol. 38, 789–793, 1989.
5. Ligthart, L. P., "A fast computational technique for accurate permittivity determination using transmission line methods," *IEEE Transactions on Microwave Theory and Techniques*, Vol. 31, No. 3, 249–254, 1983.
6. Nicholson, A. M. and G. F. Ross, "Measurement of the intrinsic properties of materials by time domain techniques," *IEEE Trans. Instrum. Meas.*, Vol. 19, 377–382, 1970.
7. Hasar, U. C., "Permittivity measurement of thin dielectric materials from reflection-only measurements using one-port vector network analyzers," *Progress In Electromagnetics Research*, Vol. 95, 365–380, 2009.
8. Hasar, U. C., "Unique permittivity determination of low-loss dielectric materials from transmission measurements at microwave frequencies," *Progress In Electromagnetics Research*, Vol. 107, 31–46, 2010.
9. Baker-Jarvis, J., *Transmission/Reflection and Short-Circuit Line Permittivity Measurements*, 1–5, National Institute of Standards and Technology, Boulder, Colorado, 1990.
10. Elmajid, H., J. Terhzaz, H. Ammor, M. Chaïbi, and A. Mediavilla, "A new method to determine the complex permittivity and complex permeability of dielectric materials at X-band frequencies," *IJMOT*, Vol. 10, No. 1, 2015.
11. Terhzaz, J., H. Ammor, A. Assir, and A. Mamouni, *Application of the FDTD Method to Determine Complex Permittivity of Dielectric Materials at Microwave Frequencies Using a Rectangular Waveguide*, Vol. 49, No. 8, Wiley, 2007.
12. Optimization Toolbox User's Guide, The MathWorks, Version 9.2, 2017.
13. Nelder, J. and R. Mead, "A simplex method for function minimization," *Computer SXSX Journal*, Vol. 7, 1965.
14. Ait Benali, L., A. Tribak, J. Terhzaz, and A. Mediavilla Sanchez, "Complex permittivity estimation for each layer in a BI-layer dielectric material at Ku-band frequencies," *Progress In Electromagnetics Research M*, Vol. 70, 109–116, 2018.